Aquat. Living Resour. 17, 1–12 (2004)

DOI: 10.1051/alr:2004004
www.edpsciences.org/alr

Aquatic
Living
Resources

Split-beam sonar observations of targets as an aid in the interpretation of anomalies encountered while monitoring migrating adult salmon in rivers

George M.W. Cronkite[1,a], Hermann J. Enzenhofer[2] and Andrew P. Gray[3]

[1] Pacific Biological Station, Department of Fisheries and Oceans, 3190 Hammond Bay Road, Nanaimo, BC V9T 6N7, Canada
[2] Cultus Lake Research Laboratory, Department of Fisheries and Oceans, 4222 Columbia Valley Highway, Cultus Lake, BC V2R 5B6, Canada
[3] Pacific Salmon Commission, 600-1155 Robson Street, Vancouver, BC V6E 1B5, Canada

Received 10 April 2003; Accepted 8 October 2003

Abstract – The experiments described in this paper relate known target configurations under controlled conditions to acoustic characteristics of multiple moving fish. We wanted to further our understanding of the interactions between targets and the effects these interactions have on the measurement of the number of salmon migrating in rivers. Multiple targets in various configurations were passed through a horizontally oriented $4° \times 10°$ beam from a split-beam echo sounder. The effects on measurements of target strength, detection probability and target location in the beam are presented. The observed target strength was not dependent on target velocity. There was a reduction in target detection due to the single-target selection criteria implemented by the hydroacoustic system. We mimicked the conditions in a river where a close range fish target may modify the beam geometry allowing detection of previously undetected targets. We demonstrated some of the effects resulting from moving targets into radial alignment and we demonstrated shadowing conditions that can cause extinction of target echoes.

Key words: Split-beam / Multiple targets / Shadowing / Interference / Target strength

Résumé – Détection de cibles par un sondeur à faisceau partagé, comme aide à l'interprétation des anomalies, rencontrées lors du suivi de la migration en rivière de saumons adultes. Les expériences, rapportées ici, décrivent des configurations de cibles connues, en conditions contrôlées du point de vue des caractéristiques acoustiques de plusieurs poissons en mouvement. Nous voulons approfondir nos connaissances sur les interactions entre cibles et les effets que ces interactions ont sur les mesures de comptage en rivière de saumons en migration. Des cibles multiples, de diverses configurations, sont passées dans le faisceau ($4° \times 10°$) d'un sondeur à faisceau partagé émettant horizontalement. Les effets sur les mesures de l'indice de réflexion, de la probabilité de détection et de la localisation de la cible dans le faisceau, ainsi que l'évolution de ces paramètres dans l'espace et le temps sont présentés. L'indice de réflexion observé dépend de la vitesse de la cible. Une diminution de la détection des cibles est observée, due aux critères de sélection de cible unique, implantés dans le système hydro-acoustique. Nous simulons les conditions en rivière, où une cible dans le champ proche pourrait modifier la géométrie du faisceau, permettant la détection de cibles non détectées antérieurement. Nous démontrons ainsi quelques effets, résultant de cibles en mouvement dans un alignement radial, ainsi que des conditions d'ombre, pouvant causer l'extinction des échos des cibles.

1 Introduction

These experiments are a continuation of our previous split-beam acoustic experiments on the interactions of controlled moving targets and the effects on target detection (Cronkite and Enzenhofer 2002). Our previous experiments indicated some of the effects of acoustic interactions between targets and have improved our ability to estimate salmon flux in rivers where multiple targets are often present in the acoustic beam. We wanted to examine certain aspects of multiple target interactions to answer questions that arose from our previous experiments and from field observations. These observations are summarised as follows:

a) We believed we noted an effect of target speed on the measured target strength in our previous experiment and we wanted to measure this relationship.
b) We have noted the loss of echoes in our field data when multiple fish are in the beam. This loss reduces the tracking algorithm's ability to track fish and therefore decreases the accuracy of the flux measurement. This loss of data can

[a] Corresponding author: CronkiteG@pac.dfo-mpo.gc.ca

occur due to interference effects between targets and due to the single-target selection criteria. We devised an experiment to isolate the effects of the single-target selection criteria by moving the targets through the beam, separated in the *X*-, *Y*- and *Z*-axes. This removed most of the shadowing effects and the small separation in *Z* allowed the single target selection criteria to be the predominant factor in data loss.

c) We have commonly noted the intermittent detection of previously undetected bottom signals in our field data and hypothesised that this was due to beam distortion by fish migrating close to the transducer. We wanted to reproduce this phenomenon experimentally to see if our hypothesis was correct.

d) Our previous experiments with spherical targets revealed some of the effects of shadowing on target strength, detection probability and position measurement. We wanted to determine if these effects were consistent for freshly killed fish targets, as fish targets more closely approximate the riverine field conditions. We also looked in more detail at shadowing with spherical targets moved into radial alignment. From an acoustic perspective, we felt it was interesting to look at radial alignment of targets since salmon travelling side-by-side will be in radial alignment for a portion of their trajectory through the beam.

We present 5 categories of experiments that were prompted by the above observations: 1) measurements of target strength, detection probability and position error for various target types to provide a baseline for comparisons; 2) effects of target speed on measured target strength; 3) effects of the single target selection criteria on the detection of multiple targets in the beam; 4) reproduction of the geometry that causes a previously undetected target to be detected; 5) effects of shadowing for fish and artificial targets.

2 Materials and methods

2.1 Study area

The experiments were performed in the same manner as that detailed in Cronkite and Enzenhofer (2002) at Cultus Lake, 90 km east of Vancouver, British Columbia, Canada. We chose the lake outlet for our experiments because it had a rectangular swimming area that was surrounded by a boardwalk, which allowed the deployment of the split-beam system and targets. There was sufficient water depth to operate a fixed-location elliptical transducer aimed in a side-looking configuration to a range of approximately 20 m. We operated the acoustic system in a manner similar to the configuration used for riverine applications, where the attainable range is limited by the return signal from the water surface and/or the bottom substrate. A string and pulley target suspension system (Cronkite and Enzenhofer 2002) allowed us to control depth, horizontal position and motion of targets in the beam.

2.2 Acoustic data collection

We set the experimental acoustic data collection parameters to the same values as those we use to measure salmon flux in rivers. These are detailed in Cronkite and Enzenhofer (2002) except that a newer model of acoustic system was used for this experiment. As a result, some of the operating parameters of the system differed, and are detailed here.

We used a Hydroacoustic Technology Inc. (HTI) Model 244 Digital Split-Beam Hydroacoustic System (HTI 2000) operating at 200 kHz, and a 4° × 10° elliptical transducer with 27 dB re 1 W efficiency. The source level was 216.47 dB and the receive sensitivity was −168.41 dB with an additional −18 dB user selectable gain. The transmitted pulse width was 0.2 ms with a pulse repetition rate of 10 pings per second. We used a pulse acceptance window between 0.1 and 0.3 ms and echoes with peak amplitude below 150 mV, or equivalently a target strength of −46.5 dB on axis, were rejected. Off-line tracking and editing of data files produced by the acoustic system were done using the Pacific Salmon Commission's FishTrack software (Xie 1999; Xie 2000).

The manufacturer calibrated the system in March 2001. In addition, an in situ target calibration was performed using a 38.1 mm tungsten carbide sphere, which produces nominal target strength (*TS*) of −39.5 dB in freshwater (MacLennan and Simmonds 1992) and for which we observed a target strength of −39.1 dB on axis (Table 1). The in-situ calibration included mapping of the beam effect in the *X*-axis direction. The cut-off in beam-angle for accepting echo data was set to ±8° in *X* and ±3° in *Y* allowing the acceptance of echo data beyond the nominal beam width of 4° by 10°.

High-resolution, unthresholded digital echo data were sampled at 12 kHz and stored on DAT tapes during the experiments. HTI provided the proprietary software that is required to read and resample these data at 48 kHz, and to write the results in ASCII files. Our analyses were based on the sum channel voltage data that are included in these files. We refer to these data as the sample data. It is these sample data that allow us to study in detail the effects of voltage thresholding, single-target selection, and other processing steps that are implemented in the echosounder.

2.3 Experimental design

The experimental design was the same as that described in Cronkite and Enzenhofer (2002). We collected acoustic data from November 1 to 8, 2001, from stationary and moving targets with a split-beam transducer affixed to a piling at the narrow end of the rectangular swimming area. The beam was aligned so that bottom and surface signals did not exceed our minimum detection threshold at a maximum range of about 20 m. This type of beam alignment allows the side-aspect detection of fish and is similar to that commonly used to observe fish migration in rivers. Single or double target configurations with pre-measured spacing in the *X*-, *Y*-, and *Z*-directions (Table 1) were moved through the acoustic beam. We will hereafter refer to each target passage through the beam as an event. A target configuration consisted of some combination of three target types; a) a 38.1 mm diameter tungsten carbide sphere (theoretical $TS = -39.5$ dB, MacLennon and Simmonds 1992), b) a 10 cm diameter lead filled plastic sphere (Kieser et al. 2000) that produces echoes of similar target strength as an adult salmon (−32 dB) and, c) freshly killed

Table 1. Statistics from target configurations passed through the 4° × 10° beam of the 200 kHz split-beam system at Cultus Lake. *X* and *Y* are horizontal and vertical target separation respectively and *Z* is distance from the transducer.

Cat.	Exp. No.	Number of events	Mean range, metres	Target configuration	Mean target strength and (SD)[a] in dB[b]	Mean detection probability (P_d) and (SD)	Position error in *X*, degrees	Position error in *Y*, degrees	Position error in *Z*, metres
1	1	9	13.98	Stationary standard sphere, axis (0°*x*, 0°*y*)	−39.1 (0.3)	1.0 (0.00)	0.47	0.20	0.01
1	1	7	13.85	Stationary standard sphere, (−2°*x*, 0°*y*)	−38.8 (0.1)	0.95 (0.03)	0.33	0.17	0.01
1	1	9	13.86	Stationary standard sphere, (−4°*x*, 0°*y*)	−39.1 (0.4)	0.78 (0.14)	0.45	0.20	0.01
1	1	24	13.88	Stationary standard sphere, (−5°*x*, 0°*y*)	−40.0 (0.6)	0.49 (0.25)	0.44	0.24	0.01
1	1	7	13.83	Stationary standard sphere, (+2°*x*, 0°*y*)	−38.0 (0.3)	0.96 (0.02)	0.29	0.26	0.01
1	1	7	13.82	Stationary standard sphere, (+4°*x*, 0°*y*)	−38.0 (0.5)	0.95 (0.05)	0.41	0.21	0.02
1	1	11	13.84	Stationary standard sphere, (+5°*x*, 0°*y*)	−38.6 (0.3)	0.76 (0.19)	0.44	0.20	0.01
1	2	8	13.89	Stationary plastic sphere, axis	−33.2 (0.3)	1.0 (0.00)	0.14	0.14	0.01
1	3	9	12.11	Stationary salmon, axis	−25.1 (0.1)	1.0 (0.00)	0.07	0.12	0.01
2	4a	20	13.97	0.2 to 0.3 m s^{-1} moving standard sphere	−38.8 (0.4)	0.86 (0.04)	0.72	0.35	0.02
2	4b	20	13.97	0.3 to 0.6 m s^{-1} moving standard sphere	−38.6 (0.4)	0.89 (0.06)	0.86	0.35	0.03
2	4c	20	13.99	0.6 to 1.0 m s^{-1} moving standard sphere	−38.4 (0.3)	0.83 (0.09)	0.86	0.35	0.03
2	5a	20	13.88	0.2 to 0.3 m s^{-1} moving plastic sphere	−32.8 (0.2)	0.96 (0.02)	0.37	0.25	0.06
2	5b	20	13.88	0.3 to 0.6 m s^{-1} moving plastic sphere	−32.8 (0.2)	0.97 (0.02)	0.33	0.23	0.05
2	5c	20	13.88	0.6 to 1.0 m s^{-1} moving plastic sphere	−32.7 (0.3)	0.96 (0.03)	0.32	0.26	0.04
3	6a	20	14.73	Moving plastic −*X*, *Y* & 0.65 m *Z*, close	−32.2 (0.3)	0.92 (0.05)	0.54	0.33	0.04
3	6b	20	15.36	Moving plastic −*X*, *Y* & 0.65 m *Z*, far	−31.9 (0.6)	0.91 (0.06)	0.44	0.27	0.04
3	7a	17	15.18	Moving plastic −*X*, *Y* & 0.15 m *Z*, close	−32.6 (1.1)	0.58 (0.28)	0.34	0.28	0.02
3	7b	17	15.35	Moving plastic −*X*, *Y* & 0.15 m *Z*, far	−31.0 (0.6)	0.76 (0.09)	0.62	0.42	0.05
4	8	4	12.22	Ghost plastic sphere	−37.0 (1.3)	0.14 (0.14)	0.48	0.39	0.02
5	9a	6	2.44	close fish – start (5.4°*x*, 0.6°*y*) [c]	−32.7 (0.6)	1.0 (0.00)	0.09	0.04	0.00
5	9b	7	2.50	close fish moved 0.1 m towards (−*X*) [c]	−41.4 (1.2)	0.90 (0.12)	0.25	0.12	0.01
5	9c	4	2.45	close fish moved 0.2 m towards (−*X*) [c]	−35.3 (0.4)	1.0 (0.00)	0.20	0.05	0.01
5	9d	4	2.44	close fish moved 0.3 m towards (−*X*) [c]	−35.4 (0.8)	0.31 (0.22)	0.14	0.08	0.00
5	9e	9	2.47	close fish moved 0.4 m towards (−*X*) [c]	−25.5 (0.4)	0.96 (0.05)	0.06	0.03	0.00
5	9f	3	2.47	close fish moved 0.5 m towards (−*X*) [c]	−25.2 (0.1)	1.0 (0.00)	0.25	0.04	0.00
5	9g	4	2.47	close fish moved 0.6 m towards (−*X*) [c]	−25.6 (0.1)	1.0 (0.00)	0.05	0.01	0.00
5	9h	6	2.47	close fish moved 0.7 m towards (−*X*) [c]	−34.4 (0.2)	1.0 (0.00)	0.08	0.04	0.00
5	9i	1	NA	close fish out of beam [c]	NA	NA	NA	NA	NA
5	9j	6	12.18	stationary plastic – start (−2.8°*x*, −0.1°*y*)[d]	−31.5 (0.5)	1.0 (0.00)	0.22	0.09	0.00
5	9k	7	12.19	stationary plastic [d]	−31.9 (0.3)	1.0 (0.00)	0.09	0.06	0.00
5	9l	4	12.19	stationary plastic [d]	−31.5 (0.2)	1.0 (0.00)	0.15	0.08	0.00
5	9m	4	12.17	stationary plastic [d]	−42.7 (0.8)	0.75 (0.24)	0.52	0.32	0.01
5	9n	1	NA	stationary plastic [d]	extinct	NA	NA	NA	NA
5	9o	3	11.98	stationary plastic [d]	−45.0 (0.7)	0.15 (0.05)	0.29	0.32	0.01
5	9p	1	NA	stationary plastic [d]	extinct	NA	NA	NA	NA
5	9q	6	12.19	stationary plastic [d]	−39.1 (0.5)	1.0 (0.00)	0.35	0.19	0.01
5	9r	7	12.18	stationary plastic [d]	−32.3 (0.4)	0.96 (0.04)	0.09	0.06	0.01
5	10a	9	11.91	Close Aligned Plastic Sphere	−32.5 (0.4)	0.87 (0.06)	0.12	0.16	0.00
5	10b	9	14.45	Far Aligned Plastic Sphere	−36.0 (1.3)	0.30 (0.16)	0.11	0.26	0.01
				note: aligned = −0.75 to −0.25 degrees in *X*					

Table 1. Continued.

Cat.	Exp. No.	Number of events	Mean range, metres	Target configuration	Mean target strength and (SD)[a] in dB[b]	Mean detection probability (P_d) and (SD)	Position error in X, degrees	Position error in Y, degrees	Position error in Z, metres
5	11a	5	12.12	Close fish stationary – aligned [e]	−26.3 (2.5)	1.00 (0.02)	0.21	0.12	0.01
5	11b	5	12.11	Close fish stationary [e]	−25.3 (0.8)	1.00 (0.00)	0.07	0.07	0.01
5	11c	10	12.11	Close fish stationary [e]	−25.4 (0.4)	1.00 (0.00)	0.04	0.08	0.01
5	11d	8	12.13	Close fish stationary [e]	−26.9 (1.2)	0.99 (0.03)	0.10	0.10	0.01
5	11e	8	12.13	Close fish stationary [e]	−28.3 (1.6)	0.99 (0.02)	0.10	0.13	0.01
5	11f	6	12.11	Close fish stationary [e]	−29.0 (0.4)	1.00 (0.00)	0.08	0.14	0.01
5	11g	10	12.14	Close fish stationary [e]	−28.7 (1.3)	0.99 (0.04)	0.12	0.15	0.01
5	11h	5	12.11	Close fish stationary – aligned [e]	−31.5 (2.5)	0.99 (0.02)	0.20	0.27	0.01
5	11i	5	15.35	Far fish moving in steps – aligned [f]	−41.4 (1.6)	0.56 (0.29)	0.54	0.63	0.03
5	11j	5	15.37	Moved 0.1 m to $-X$ from aligned [f]	−44.0 (0.6)	0.64 (0.26)	0.50	0.29	0.02
5	11k	10	15.40	Moved 0.2 m to $-X$ from aligned [f]	−37.0 (0.6)	1.00 (0.01)	0.22	0.17	0.01
5	11l	8	15.41	Moved 0.3 m to $-X$ from aligned [f]	−29.1 (0.4)	1.00 (0.00)	0.12	0.11	0.01
5	11m	8	15.38	Moved 0.3 m to $+X$ from aligned [f]	−33.9 (1.4)	1.00 (0.00)	0.21	0.28	0.01
5	11n	6	15.38	Moved 0.2 m to $+X$ from aligned [f]	−36.3 (1.6)	0.99 (0.01)	0.26	0.40	0.01
5	11o	10	15.34	Moved 0.1 m to $+X$ from aligned [f]	−41.1 (1.1)	0.88 (0.11)	0.49	0.41	0.02
5	11p	5	15.39	Far fish moving in steps – aligned [f]	−42.6 (0.6)	0.17 (0.11)	0.66	0.78	0.03

(a) Standard deviation calculated from the event-wise estimates.
(b) Calculated from the mean backscattering cross section.
(c) The fish target is moved in discrete 0.1 m steps while the corresponding longer-range plastic sphere [d] is stationary in the beam, e.g. Exp. No. 9a pairs with 9j, 9b with 9k, etc.
(d) The longer-range plastic sphere is stationary in the beam while the corresponding fish target [c] is moved in discrete 0.1 m steps, e.g. Exp. No. 9j pairs with 9a, 9k with 9b, etc.
(e) The closer-range fish target is stationary in the beam while the corresponding longer-range fish target [f] is moved in discrete 0.1 m steps in and out of alignment in the X-direction indicated, e.g. Exp. No. 11a pairs with 11i, 11b with 11j, etc.
(f) The longer-range fish target is moved in discrete 0.1 m steps in and out of alignment in the X-direction indicated while the corresponding closer-range fish target [e] is stationary in the beam, e.g. Exp. No. 11i pairs with 11a, 11j with 11b, etc.

coho salmon (*Oncorhynchus kisutch)*. The coho salmon targets exhibited *TS* values of approximately −25 dB but displayed slow changes in *TS* likely due to the amount of air contained in the swim bladder. We noted the release of bubbles from the mouths of the dead salmon at various times during the experiments, from which we infer that the volume of air in the air bladder slowly decreased.

Horizontal alignment and synchronous movement of the targets was achieved by suspending them from a 3 m wooden dowel hanging from two pulleys that ran along guy lines above the water surface. Variations of the target's speed in the X-direction were achieved by varying the rate at which the ropes attached to the wooden dowel were pulled by an assistant. The assistant pulled the targets through the beam at constant velocity throughout each event. The targets could also be moved vertically with monofilament lines that passed through pulleys on the wooden dowel and connected to fishing reels mounted on the boardwalk. Horizontal and vertical movements of the targets were measured with tape measures also mounted on the boardwalk.

Salmon targets were suspended with three monofilament lines from the wooden dowel to the dorsal surface of the fish. One line ran diagonally from the fish's nose, forward to the front of the wooden dowel and the remaining lines were attached to the base of the dorsal fin and the adipose fin respectively. This configuration allowed the fish to hang and travel perpendicular to the beam axis.

We lowered a plastic sphere down through the beam at approximately 12 m range, until the point at which the target echo amplitude, as observed on the oscilloscope screen, was below the threshold level of 150 mV. At this point the target was not detected by the acoustic system. We then moved a freshly killed salmon headfirst through the beam at approximately 2.5 m range from the transducer. This configuration approximates a common situation in the riverine environment where the transducer is aimed down until the substrate echo signal is slightly below the threshold set for the acoustic system. When salmon migrate through the beam close to the transducer, a ghost target can appear (Enzenhofer and Cronkite 2000).

Three experiments were performed to determine the effects of moving targets into radial alignment. We define radial alignment as the point at which two targets are aligned one behind the other with respect to the approaching acoustic wave front. We used a stationary plastic sphere at approximately 12 m range and a salmon at approximately 2.5 m range, with the

salmon moving in steps of 0.1 m into radial alignment with the plastic sphere. This procedure was replicated using two salmon targets located at approximately 12 m and 15 m range with the closer salmon remaining stationary and the farthest salmon moving in steps of 0.1 m. We also used two plastic spheres, the closer at approximately 12 m range and the farthest at approximately 14.5 m range. The farthest target was passed back and forth in the *X*-direction, behind the stationary closer target. This positioned the targets in repeated radial alignment during each event.

Eleven distinct experiments were performed and the results are listed in Table 1. The experiments include acoustic measurements of: 1) a stationary standard sphere at 14 m range; 2) a stationary plastic sphere at 14 m range; 3) a stationary freshly killed coho salmon at 12 m range; 4) a standard sphere moving at speeds between 0.2 and 1 m s^{-1} in the *X*-direction; 5) a plastic sphere moving at speeds between 0.2 and 1 m s^{-1} in the *X*-direction; 6) plastic spheres moving in the *X*-direction while separated in *X*, *Y* and 0.65 m in *Z*; 7) plastic spheres moving in the *X*-direction while separated in *X*, *Y* and 0.15 m in *Z*; 8) the ghost target effect with a stationary plastic sphere at 12 m range and a freshly killed salmon target moving in the *X*-direction at 2.5 m range; 9) a stationary plastic sphere located at 12 m range with a freshly killed salmon moving in steps of 0.1 m through the beam at 2.5 m range; 10) a stationary plastic sphere at 12 m range with a second plastic sphere at 14.5 m range moving back and forth through radial alignment; 11) a stationary freshly killed salmon at approximately 12 m range and a second salmon at approximately 15.5 m range moving through radial alignment in steps of 0.1 m.

2.4 Data analyses

A least squares regression was fitted to the *X* vs. time, *Y* vs. time and *Z* vs. time angular position data for all of the target configurations to estimate measurement error in the position data. The *X*-, *Y*- and *Z*-co-ordinate residuals were calculated and the standard deviation of these residuals gave the position measurement error in degrees (Table 1) to allow comparisons of position error between targets at different ranges. Target strength is also listed in Table 1 and is calculated from the mean backscattering cross section, $\overline{\sigma}$, according to the following definition (Foote 1987): $\overline{TS} = 10 \log (\overline{\sigma}/4\pi)$ and is applied within events. The detection probability (P_d) represents the number of return echoes divided by the number of pings transmitted between the first and last times of target detection within an event. The data are summarised by events to simulate fish moving through the beam in a typical riverine configuration.

To test the effects of target speed on the measured *TS* we first determined the range of received echo scatter in the *X*-direction for the stationary plastic sphere to be ±0.25° when on-axis. We then calculated the speeds of the moving targets using the lengths of the smoothed trajectories over time for the full track lengths. Then we analysed the *TS* values for the moving targets for only those echoes received within ±0.25° of the axis in the *X*-direction. This allowed data from the stationary targets on the beam axis to be included in the analyses, as the complete data set was then taken from the same region in the beam to compensate for possible beam effects. We then fit standard regressions on *TS* vs. speed and speed vs. *TS*. Because there was error in the measurement of both *TS* and speed, these regressions should provide the upper and lower bounds for the true relationship. The slope for the true relationship must exist somewhere between these two extremes. We then bootstrapped 1000 replicates and plotted the distributions of possible slopes with the 95% confidence intervals (Efron and Tibshirani 1993). If the 95% confidence intervals of the slopes did not include 0 or ∞, then we would infer that the relationship was significant. The data were checked for normality by using quantile-quantile plots (S-PLUS 2000, 1999) of the residuals of the fitted values, and linearity, by plotting the Lowess smoothed relationships (Chambers et al. 1983). If the quantile-quantile plots were nearly linear then the data was determined to be Gaussian and if the Lowess smoothed plots were nearly linear then the data was determined to have a linear relationship.

3 Results

3.1 Measurements of *TS*, P_d and position error for various target types

The stationary reference targets used in this experiment are summarised in Table 1, Exps. 1–3. Stationary reference targets include the standard target, the plastic sphere and a freshly killed salmon. The *TS* of the various off-axis positions for the standard target varied by approximately ±1 dB from the on-axis position, and did not show signs of systematic change towards the beam edges, indicating that the echosounder's algorithms correcting for the beam effect were working acceptably.

The standard target and plastic spheres maintained a constant *TS* value throughout the experiments but the salmon exhibited changes in *TS* over time, likely due to the release of air bladder gasses. This variation in *TS* did not affect the results of the experiments where salmon were being used, as the variation with time was slow and therefore the *TS* was approximately constant during each experiment.

3.2 Effects of target speed on measured *TS*

Differences were apparent in the *TS*, P_d and position error in *X*, *Y*, and *Z* for the stationary (Table 1, Exps. 1, 2) and moving (Exps. 4a-c, 5a-c) reference targets. Ping to ping variation in *TS* is always present for moving targets but we also thought there may be a systematic component to this effect (see Cronkite and Enzenhofer 2002). Figure 1a presents the scatter plot of *TS* vs. speed for the standard sphere and Figure 1b presents the same plot for the plastic sphere. The lines on each plot represent the regression assuming that all of the error is in the *TS* measurement (dashed) and assuming all of the error is in the speed measurement (solid). The true relationship lies somewhere between these two lines. Figure 2 presents the frequency histograms of the bootstrapped slopes (1000 replicates) which were used to determine if the 95% CIs

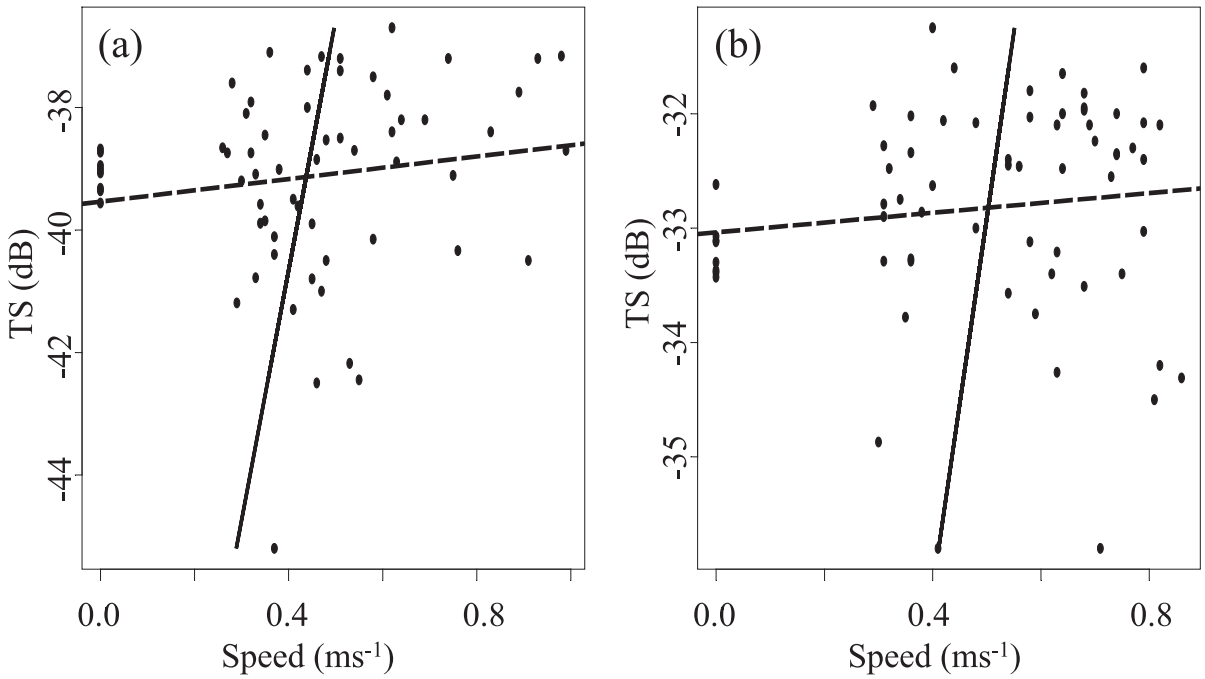

Fig. 1. The relationship between *TS* and target speed for (a), the standard sphere and (b), the plastic sphere. The dashed lines represent the regression lines assuming that all of the error is in the *TS* measurement and the solid lines assume all of the error is in the speed measurement. Note the difference in scales for the *Y*-axis.

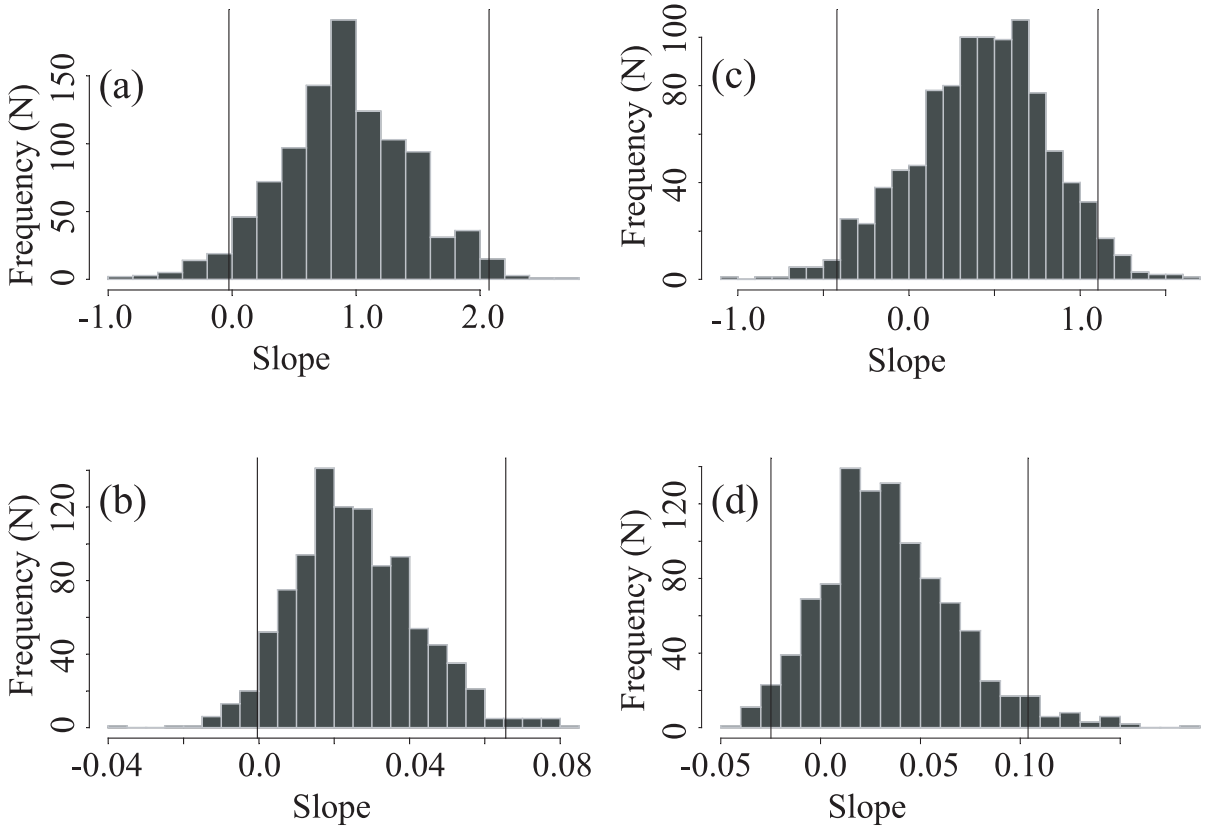

Fig. 2. Frequency histograms (based on 1000 replicates) of boot-strapped estimates of slope coefficients for *TS* vs. speed and speed vs. *TS* regressions showing that the observed *TS* was not a function of target velocity. (a) Is from the standard target with all error assumed in the *TS* measurement and (b) is from the standard target with all error assumed in the speed measurement. (c and d) Are the same respectively for the plastic sphere. The vertical lines represent the 95% confidence intervals.

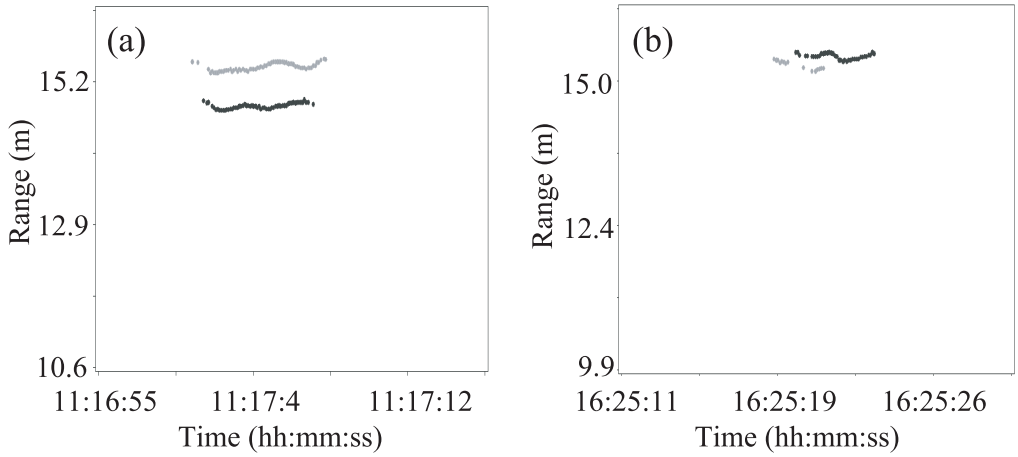

Fig. 3. (a) Echogram of an event where the targets are separated by 0.5 m in *X* and *Y* and 0.65 m in *Z* with the shorter-range target being located closer to the top (positive *Y*) edge of the beam. (b) Echogram of an event with the same *X* and *Y* separation but with *Z*-separation reduced to 0.15 m.

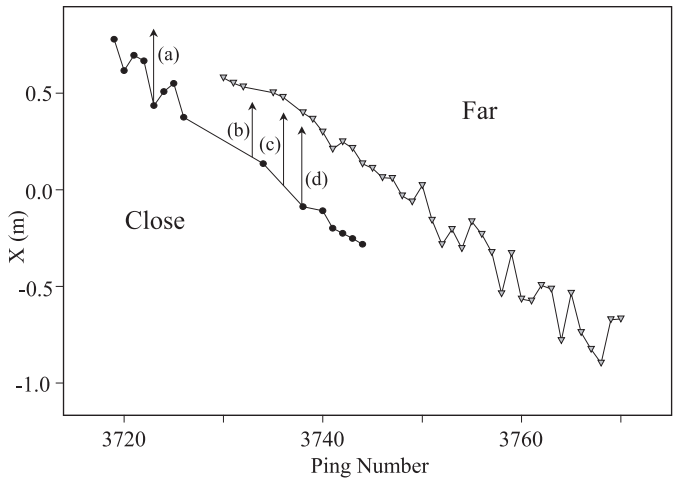

Fig. 4. *X*-position vs. ping data for both the closer- and farther-range targets shown in Figure 3b. The vertical arrows indicate pings where (a) only the close target was detected, (b) neither target was detected, (c) only the far target was detected, and (d) both targets were detected.

included slopes = 0 or ∞ (values that indicate no systematic dependence of *TS* on speed or speed on *TS*, respectively).

The standard target and plastic spheres were detected off-axis to approximately ±6° in the *X*-direction as they were moved through the beam. The acoustic system was set to accept data out to ±8° in the *X*-direction, indicating that the targets were no longer detected at the edges of the beam due to the threshold set for these experiments and not due to a selected truncation of the beam boundary.

3.3 Effects of the single target selection criteria on the detection of multiple targets in the beam

We modified some of the target experiments performed in our previous work to look at the effects of two moving targets that are not shadowing each other as they pass through the beam. Figure 3a presents an event where the targets are separated by 0.5 m in *X* and *Y* and 0.65 m in *Z* with the shorter-range target located closer to the top (positive *Y*) edge of the beam. This separation of the targets in three axes was an attempt to remove the shadowing seen with radially aligned targets that affects the acoustic detection of the shadowed target. Both the shorter- and longer-range targets for this event displayed the characteristics of isolated single-targets without any apparent effects on *TS* or P_d (Table 1, Exps. 6a, b). Figure 3b presents an event with reduced separation in *Z*. The targets are separated by 0.5 m in *X* and *Y* and 0.15 m in *Z*, again with the shorter-range target being closer to the top of the beam. When the *Z*-distance was reduced from 0.65 m to 0.15 m, we recorded a significant decrease of 0.34 in the P_d for the closer-range target (two-sample *t*-test, $\alpha = 0.05_{2\,\mathrm{tail}}$: $t = 5.52$; $df = 16$; $p = 0$), along with an increase of 0.8 dB in the standard deviation of the *TS* (Table 1, Exps. 6a and 7a). The longer-range target showed a significant increase in *TS* of 1.8 dB (two-sample *t*-test, $\alpha = 0.05_{2\,\mathrm{tail}}$: $t = 11.00$; $df = 20$; $p = 0$) when compared with an isolated moving target travelling at approximately the same speed (Table 1, Exps. 5b and 7b). Figure 4 displays *X*-position vs. ping for both the shorter- and longer-range targets shown in Figure 3b. The movement in the *X*-direction was systematic throughout the event for both targets.

Figure 5 displays the echo amplitude from the 48 kHz sample data for the pings labelled (a) to (d) in Figure 4. Except for its relatively low peak height, an ideal target detection scenario is presented for the echo from the closer target (Fig. 5a). It is characterised by a symmetric peak of appropriate duration, with both sides falling below the threshold. The farther target is below the threshold and remains undetected. Two distinct peaks are present in the remaining three plots, but these present three quite different scenarios to the peak detection algorithm in the echo sounder. Starting with Figure 5d both peaks clearly should be and are detected as both peaks are of sufficient height, appropriate width and fall on both sides below the threshold. Both peaks in Figure 5b remain undetected,

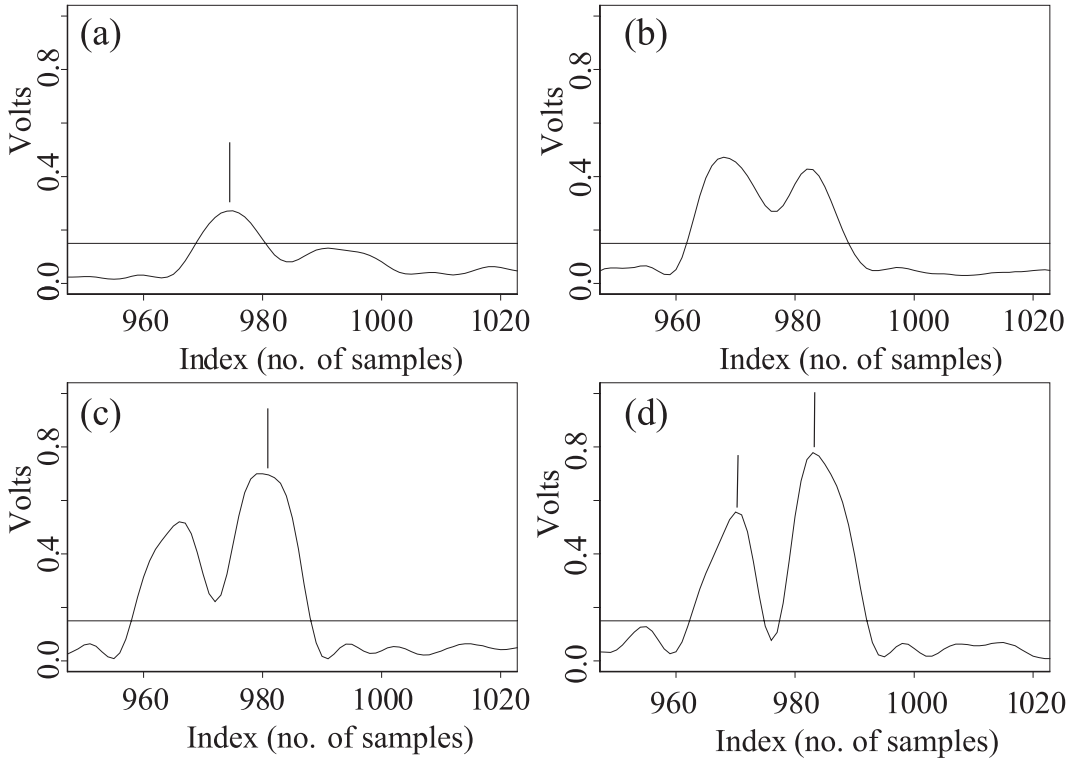

Fig. 5. 48 kHz sample data from pings (a)–(d) in Figure 4. The *X*-axis range is centred at the targets, the label "Index" refers to the number of 48 kHz samples from the start of the ping. The detected peaks are marked with vertical lines.

as the saddle between them is not low enough to be recognised by the peak detection algorithm. These peaks are therefore seen as one peak that exceeds the 0.1 to 0.3 ms window and are rejected. Finally, the saddle between the first and second peak in Figure 5c is low enough to allow the detection of the peaks by the peak detection algorithm, but only the higher peak is accepted because the saddle does not pass below the threshold. The lower peak is dismissed as a maximum of one peak is assigned each time the echo rises above and falls below the threshold.

3.4 Reproduction of the geometry that causes a previously undetected target to be detected

Figure 6 shows the effects of a close range salmon target on a normally undetected plastic sphere at longer range. As the salmon was passed through the beam, the plastic sphere was detected intermittently during the time the salmon was in the beam. We refer to this previously undetected target as a ghost target. There was a secondary ghost target detected at farther range than the plastic sphere, which we believe was the return signal from aquatic weeds that were growing on the lake bottom at that range. We measured a significant decrease of 4 dB in the *TS* of the ghost target when compared with the stationary plastic sphere (two-sample *t*-test, $\alpha = 0.05_{2\,\text{tail}}$: $t = -6.06$; $df = 3$; $p = 0$) (Table 1, Exps. 8, 2). The *XY* angular position information was also incorrect when compared with the true position of the ghost target in the beam.

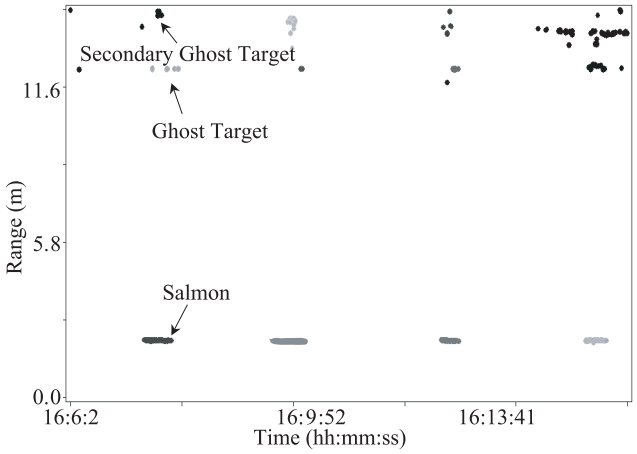

Fig. 6. Echogram showing the effects of a salmon target on an otherwise undetected target at farther range. The plastic sphere (ghost target) was detected when the salmon was passed through the beam. An additional target at farther range was also detected at these times.

3.5 Effects of shadowing for fish and artificial targets

A plastic sphere was positioned at approximately 12 m range near the beam axis and a salmon target was moved in steps of 0.1 m through the beam at approximately 2.5 m range. *TS* and P_d for the stationary plastic sphere were affected (Table 1, Exps. 9j-r). The plastic sphere demonstrated near normal *TS* and P_d as long as the salmon was essentially

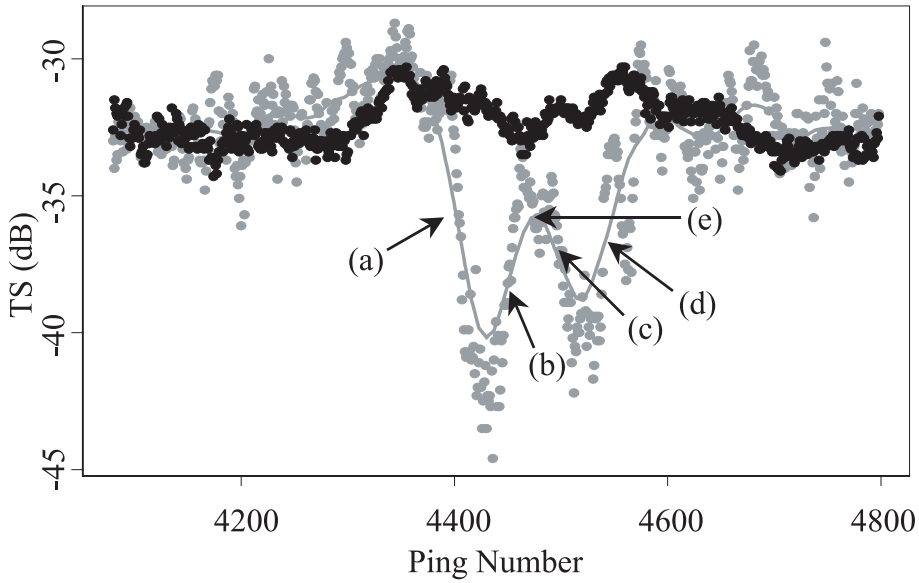

Fig. 7. Effects of radial alignment of two plastic sphere targets on *TS*. Two distinct dips in *TS* are seen as the target at 14.5 m range (grey points) moves through radial alignment with a stationary target at 12 m range (black points). The grey line represents the smoothed *TS* values for the farther-range target. See text for explanation of annotations (a) to (e).

outside the beam. The mean *TS* for the plastic sphere displayed a minimum as the fish target was incrementally moved through the beam. The measured *TS* of the plastic sphere decreased by more than 13 dB at one position of the fish, and the echo amplitude fell below the detection threshold at two positions.

The results for the closer range salmon target were unexpected for this experiment (Table 1, 9a–i). The mean *TS* for the salmon varied by as much as 16 dB between the maximum and minimum measurements.

Shadowing also occurs with smaller targets that are in radial alignment at longer ranges. Figure 7 presents one event in which a plastic sphere at 14.5 m range was moved into radial alignment with a stationary plastic sphere at 12 m range. The grey line shows (a), the drop in *TS* as the targets approached alignment, (b), a rise in *TS* as they come into alignment, (c), a second drop in *TS* and (d), a rise back to the original *TS* value. We made the assumption that the targets were in radial alignment at the point marked (e) in Figure 7 due to the behaviour of the *TS* curve, but we did not make a physical measurement of the point of radial alignment. Visually the targets appeared to be in alignment at point (e). The mean *TS* for the shadowed target was 3.3 dB less than that measured for the closest target for the time when the targets were within ±0.25° of assumed radial alignment (two-sample *t*-test, $\alpha = 0.05_{2\,\mathrm{tail}}$: $t = 11.21$; $df = 19$; $p = 0$). The mean *TS* standard deviation for the shadowed target was 0.9 dB higher than that measured for the closest target for the same ±0.25° of assumed radial alignment (Table 1, Exps. 10a and b). We also measured a significant decrease in the P_d of 0.57 for the shadowed target when in radial alignment (two-sample *t*-test, $\alpha = 0.05_{2\,\mathrm{tail}}$: $t = 14.85$; $df = 19$; $p = 0$).

Similar results were obtained for two salmon moving into radial alignment in steps of 0.1 m. Table 1, 11a-h and 11i-p present the results for a stationary salmon at approximately 12 m with a second salmon moving into radial alignment in steps of 0.1 m at approximately 15.5 m. A more highly variable *TS* was measured for the closer unshadowed target along with a high P_d. The angle measurement error was greater for the closer salmon when the two salmon were aligned. The far salmon showed lower *TS* values during times of alignment (approximately −42 dB) and closer to expected *TS* values when out of alignment (approximately −29 dB). The P_d and position error followed patterns similar to those observed for the plastic spheres: low detection along with larger position error in *X*, *Y* and *Z* for the shadowed target during times of radial alignment.

We also compared the acoustically measured position of the far fish with the "true position". The true position of the far fish was obtained by aligning the fish at the beam centre and recording the pull-rope position at each 0.1 m step. Figure 8 presents the acoustic angle vs. the mechanical angle of the fish and shows an increase in the *X*-angle error as the far-range salmon moved further off axis. The black line is the one-to-one line and represents perfect agreement between the measured acoustic position and the true position.

4 Discussion

4.1 Measurements of *TS*, P_d and position error for various target types to provide a baseline for comparisons

One consideration when using plastic spheres and tungsten carbide spheres is the potential difference between the acoustic attributes of these targets compared to that of fish in the wild. In this study we used both artificial targets and freshly killed coho salmon to determine if the results for artificial targets also held true for salmon. We must also consider that a freshly killed salmon will not give the same results as a live

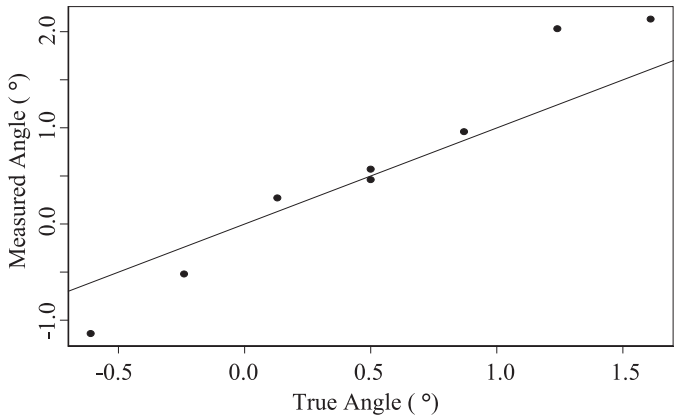

Fig. 8. Acoustically measured *X*-position and the true *X*-position of a farther-range salmon target. Position measurements are in degrees off-axis.

salmon but the results may be more representative of migrating salmon than those from an artificial target.

4.2 The effects of target speed on measured *TS*

There was variation in the measured *TS* as our spherical targets were moved through the beam and we thought that the *TS* might be dependent on the target's speed of travel. However, since the 95% CI's of the frequency histograms of bootstrapped slopes (Fig. 2), include slopes = 0, we conclude that *TS* was not dependent on the target velocity for the range of velocities tested. In a previous experiment we obtained a negative bias in *TS* for a moving target when compared with a stationary target (Cronkite and Enzenhofer 2002). We are unable to explain this difference in the results, but we believe that the results from the current experiment are representative, as this experiment was designed specifically to test the previous observation. We have noted a large variation in *TS* in our salmon field data from the Fraser River and this variation has been documented by other researchers such as Fleischman and Burwen (2000). This *TS* variation is likely due to the salmon's orientation in the beam. We measured an increase in the position error and a decrease in the P_d for the moving targets, which is to be expected due to the movement of the target through varying levels of detection in the beam.

4.3 Effects of the single-target selection criteria on the detection of multiple targets in the beam

We found that two targets separated by 0.65 m in *Z* did not display interference effects and were detected as two distinct, single targets as they passed through the beam. If the spacing was reduced to 0.15 m in *Z* (which is approximately equal to half of the pulse width, $0.5c\tau$), but the spacing in *X* and *Y* maintained, then interference effects were measured. We demonstrated that these effects were due to the single-target selection criteria that is used in the echosounder rather than by acoustic shadowing between the targets. This is highlighted in Figures 5b and 5c, where the echo amplitude between peaks does not fall below the echo sounder's peak separation threshold or the echo threshold respectively. This causes *TS* bias and a decrease in the P_d. The closer target in Figure 5 was largely undetected even though it was the same physical size as the detected target, because it was located closer to the edge of the beam and thus generated lower echo amplitudes. Peak detection could possibly be improved or even optimised for this situation by using different threshold and peak-width parameters, however, little can be done beyond this as other parameters and features of the peak detection algorithm are coded into the echo sounder and thus are inaccessible to the user. The single-target selection criteria are useful to isolate single-targets when *TS* values are desired. However, in the riverine environment it is often necessary to measure salmon fluxes when the salmon are separated by 0.15 m or less, which is equal to, or less than, the theoretical minimum separation distance to allow discrimination.

4.4 Reproduction of the geometry that causes a previously undetected target to be detected

When a large target such as a salmon passes through the acoustic beam at close range it will have a modifying effect on the beam because the salmon takes up a large portion of the beam cross-section and therefore will not have the characteristics of a point-source target. Targets that are at a longer range than the salmon may experience a weaker or stronger acoustic field and thus may appear to be "shadowed" or appear stronger. Thus, previously undetected targets may appear. We refer to these targets as ghost targets. Our experiment allowed us to establish the geometry needed to make this effect occur. The result replicates our observations in the riverine environment where we detect the bottom signal intermittently when fish pass through the beam within the first few metres of range. When fish are not present, the bottom signal remains below threshold. The echogram (Fig. 9) displays this effect as seen for migrating sockeye on the Nushagak River, Alaska (Don Degan, Aquacoustics, Inc., personal communication). Examples of the ghost targets are outlined with dotted circles and coincide with fish passing at closer range through the beam. These ghost targets are not artefacts of the acoustic system, but result from the disturbance of the acoustic beam by a fish, which is particularly strong when the fish fills a large fraction of the beam cross-section.

4.5 Effects of shadowing for fish targets and artificial targets

In the first shadowing experiment, the shadowed plastic sphere showed a decrease in *TS* when the salmon at closer range was in alignment. In addition, at two positions of the fish, the echoes from the longer-range plastic sphere did not pass the single-target selection criteria. This extinction of echoes is consistent with a blocking of the beam by the salmon, preventing detection of the target at longer range. The extinction of echoes by close-range fish indicates the importance of maintaining as long a range as possible between the closest detected targets and the transducer. The extinction effect is a

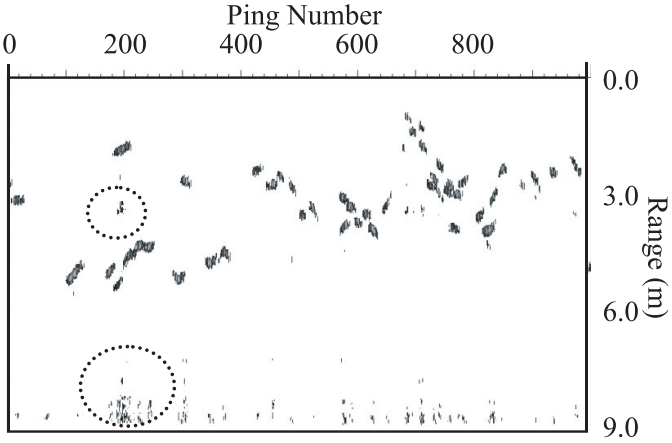

Fig. 9. Echogram of migrating sockeye on the Nushagak River, Alaska, with examples of "ghost targets" (enclosed in dotted circles) that appear when salmon pass near the transducer.

concern in the riverine environment as often fish are located very close to the transducer and our results show that short-range fish may at times not allow the detection of longer-range targets. An example is presented where we hypothesise that the gaps in the echogram are indicative of the presence of extremely close range salmon blocking the acoustic beam, leading to a loss of data (Fig. 10). This echogram also displays the ghost target effect at approximately 14 m and beyond the 28 m range, similar to that displayed in Figure 9. This echogram was recorded during high-density pink salmon flux on the Fraser River, BC on September 20, 2000. The pink salmon were visually observed to be migrating very close to the transducer, and at times swimming behind the transducer in shallow water.

We also obtained unexpected results from the experiment with the closer-range salmon and the longer-range plastic sphere. The position information for the close-range salmon was erratic and incorrect. We believe that this was due to the large salmon target being in the near-field of the transducer (or the transducer was in the near-field of the salmon), even though at 2.5 m range, it was over twice the manufacturer's rated near-field distance. This finding bears further scrutiny since it is relevant to riverine work, particularly if the ability to track these closer-range targets accurately is reduced. Dawson et al. (2000) documented degraded fish position information at close ranges in Alaskan rivers with a Biosonics acoustic system, which they hypothesised was due to the size of the salmon target relative to the beam diameter and the complex scattering nature of salmon targets.

The second shadowing experiment made use of two plastic spheres with the farther range sphere moving at a constant slow velocity back and forth through the beam. These spheres have less variable acoustic properties than fish. The results showed a negative bias in *TS* for the farther range, shadowed target along with a decrease in the P_d and some increase in angular position error in the *Y*-axis. There was an interference effect between these two targets when separated by 2.5 m in range (Fig. 7). First we see the large drop in *TS* for the farther range shadowed target followed by a rise in *TS* when the two targets become radially aligned. We hypothesise that this may be due to the narrow forward-scatter beam emanating from the closer range plastic sphere. Clay and Medwin (1977) present scattered radiation patterns for spheres in the far field, and the plot for $ka = 10$ approximately corresponds to the plastic spheres we used ($ka \approx 42$). Here, *ka* is defined as the wave number in the medium ($2\pi/\lambda$) multiplied by the radius of the sphere. The narrow forward-scatter beam becomes more pronounced as *ka* increases in value. In our example, the forward-scatter beam increases the sound energy hitting the second target and bolsters the return signal, returning more energy to the transducer. When the shadowed target is not in radial alignment, there are points at which the target would be located in the null between the main forward-scatter beam and the first side-lobe. In this position, there is a decrease in the amount of reflected energy and therefore lower *TS* measurements occur. When a farther range, shadowed target is located in this null, extinction of the echo from the farther range target can occur as we demonstrated with the salmon target at close range and the plastic sphere at farther range.

The *TS* measurement of the closer range stationary target was also affected when the two targets were radially aligned (Fig. 7). The *TS* curve appears to rise for the closer-range, stationary target at the same time as the curve drops for the farther-range, moving target. The interference between the two targets can change the detection properties of both of the targets (i.e. not just the shadowed target) as the effects result from both forward-scatter and back-scatter. Experiments with stationary spheres by Soule et al. (1995) and our own experiments with moving targets (Cronkite and Enzenhofer 2002) show that multiple targets in the beam can display either constructive or destructive interference depending on the orientation and spacing of the targets, resulting in both positive and negative biases in *TS* and P_d. In the case of Soule et al. (1995) the targets were separated by less than one-half of the pulse width ($0.5c\tau$), whereas in our current experiment we detected interference effects in both targets at separation distances much greater than $0.5c\tau$. We did not predict these effects at this large a separation distance, especially for the closer-range target.

We believe that the interference between two salmon targets moving through radial alignment is the cause of the increasing angular error as the shadowed target moves off-axis (Fig. 8). The shadowed target was detected by the acoustic system farther off-axis than was its true location by as much as 0.75°. This effect is in the opposite direction to the split-beam bias documented by Kieser et al. (2000), which showed that targets further off axis were more likely to be detected closer to the centre of the beam than was their true position. This bias became larger as the signal-to-noise ratio decreased. In our experiment, the signal to noise ratio in the lake was higher than that commonly measured in rivers, reducing the effect of the split-beam bias and increasing the relative importance of interference between the two targets. At present, we do not have similar data for two plastic spheres, as the spheres were observed only during times of continuous motion of one sphere, and not in a stepwise motion as was required for the salmon targets.

We have presented data from various target configurations that show the interference effects of shadowing and extinction. These data also show the effects interference can have on *TS* and target position measurements. We have demonstrated that

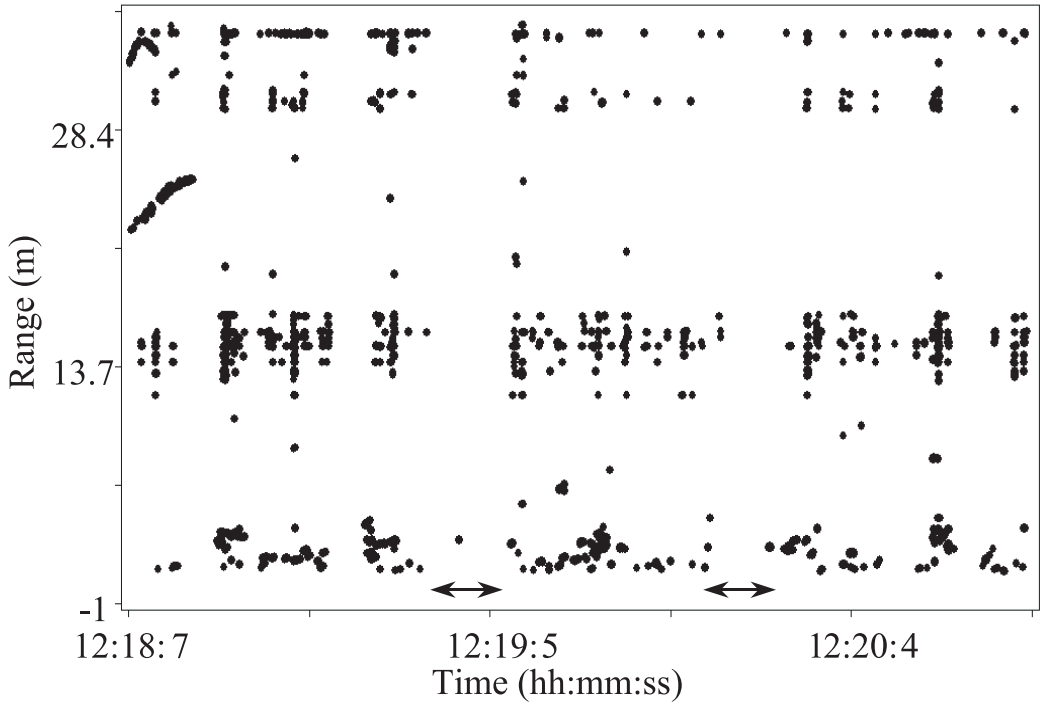

Fig. 10. Echogram of migrating pink salmon on the Fraser River, British Columbia. Targets from 0 to 7 m range are migrating pinks. Arrows mark periods of believed signal extinction due to close range migrating pinks. Ghost targets are also evident at 13.7 m range and beyond 28.4 m range.

interference effects are present when the targets are separated by one-half the pulse width or less, and also when the separation distances are much larger. In the case of the ghost targets, we demonstrated the detection of targets that were outside of the hypothetical acoustic detection volume. We were able to re-create the conditions, and therefore understand the reasons for, some of the features we have seen in our field data. We believe that these experiments demonstrate that when more than one target is present in the beam there is a need to be cautious about the data. The acoustic interactions between targets in the beam are complex and have consequences for the accuracy of the data collected.

Acknowledgements. We thank Dr. Tim Mulligan, Dr. Robert Kieser and Dr. John Holmes for their advice and constructive reviews of this paper. We also thank Rob Kronlund for his advice on the appropriateness of the statistical analysis techniques used. We also thank the three anonymous referees for their perceptive and constructive comments.

References

Chambers J.M., Cleveland W.S., Kleiner B., Tukey P.A., 1983, Graphical Methods for Data Analysis. Wadsworth, Belmont, California.

Clay C.S., Medwin H., 1977, Acoustical Oceanography: principles and applications. John Wiley and Sons, New York.

Cronkite G.M.W., Enzenhofer H.J., 2002, Observations of controlled moving targets with split-beam sonar and implications for detection of migrating adult salmon in rivers. Aquat. Living Resour. 15, 1-11.

Dawson J.J., Wiggins D., Degan D., Geiger H., Hart D., Adams, B., 2000, Point-source violations: split-beam tracking of fish at close range. Aquat. Living Resour. 13, 291-295.

Efron B., Tibshirani R.J., 1993, An Introduction to the Bootstrap. Chapman and Hall, New York.

Enzenhofer H.J., Cronkite G., 2000, Fixed location hydroacoustic estimation of fish migration in the riverine environment: an operational manual. Can. Tech. Rep. Fish. Aquat. Sci. 2312, 46.

Fleischman S.J., Burwen D.L., 2000, Correcting for position-related bias in estimates of the acoustic backscattering cross-section. Aquat. Living Resour. 13, 283-290.

Foote K.G., 1987, Fish target strengths for use in echo integrator surveys. J. Acoust. Soc. Am. 82, 981-987.

Hydroacoustic Technology Inc., 2000, Model 241/243/244 split-beam digital echo sounder system operator's manual, version 1.8. Hydroacoustic Technology Inc., Seattle, Washington.

Kieser R., Mulligan T., Ehrenberg J., 2000, Observation and explanation of systematic split-beam angle measurement errors. Aquat. Living Resour. 13, 275-281.

MacLennan D.N., Simmonds E.J., 1992, Fisheries acoustics. Chapman and Hall, London.

Soule M.A., Barange M., Hampton I., 1995, Evidence of bias in estimates of target strength obtained with a split-beam echo-sounder. ICES J. Mar. Sci. 52, 139-144.

S-PLUS 2000, 1999, Guide to statistics, volume 1. Data Analysis Products Division. MathSoft, Seattle WA, pp. 57-57.

Xie Y., 1999, A tracking and editing software package for split-beam fish sonar data: PSC split-beam fish tracker user's guide, Pacific Salmon Comm. User's Guide, p. 26.

Xie Y., 2000, A range-dependent echo-association algorithm and its application in split-beam sonar tracking of migratory salmon in the Fraser River watershed, IEEE, J. Ocean. Eng. 25, 387-398.